RSC Advances

PAPER

View Article Online
View Journal | View Issue

Cite this: *RSC Adv.*, 2019, **9**, 32425

Mono and co-immobilization of imidazolium ionic liquids on silica: effects of the substituted groups on the adsorption behavior of 2,4-dinitrophenol†

Zhike Wang,*[ab] Honglian Ge,[a] Xueyuan Wang,[b] Cunling Ye*[b] and Shunli Fan[a]

Ionic liquid modified silicas with high adsorption capacity for phenols prompt us to deeply explore the contribution of interactions between the adsorbent and adsorbate, with a particular focus on hydrophobicity, π–π, electrostatic and acid–base interactions. Herein, by introducing a series of typical substituent groups including *N*,*N*-dimethylaminopropyl (A), benzyl (B), dodecyl (D) and naphthylmethyl (N) in an imidazole ring (Im), three mono-immobilized and two co-immobilized imidazolium ionic liquid modified silicas, namely SilprAImCl, SilprBImCl, SilprNImCl, SilprDBImCl and SilprDAImCl, werre synthesized for removal and recovery of 2,4-dinitrophenol (2,4-DNP) from aqueous solutions. Adsorption kinetics, isotherms, thermodynamic analysis and desorption experiments have been carried out. The experimental results reveal that the substituent groups such as *N*,*N*-dimethylaminopropyl, benzyl and naphthylmethyl on the imidazole ring can significantly enhance the adsorption of 2,4-DNP *via* the acid–base interaction or π–π interaction and the adsorption capacity of 2,4-DNP follows the order: SilprNImCl > SilprAImCl > SilprBImCl. Furthermore, SilprDBImCl exhibits the largest adsorption capacity and SilprDAImCl has the lowest among the five adsorbents. These interesting finds indicate that the combination of hydrophobicity and π–π interactions lead to enhanced adsorption performance towards 2,4-DNP, while the combination of the hydrophobicity and acid–base interactions can restrain greatly adsorption of 2,4-DNP from aqueous medium. Adsorption mechanisms of 2,4-DNP on the five adsorbents have been clarified. These results will provide a deeper insight for efficient removal of phenols from water environments.

Received 20th September 2019
Accepted 2nd October 2019

DOI: 10.1039/c9ra07635b

rsc.li/rsc-advances

1. Introduction

2,4-Dinitrophenol (2,4-DNP), a priority pollutant, is widely acknowledged to be detrimental to human health and the environment. The water pollution resulting from 2,4-DNP is considered as a general problem. Many methods have been proposed to remove the 2,4-DNP from aqueous solutions including advanced oxidation,[1] electrochemical oxidation,[2–4] biodegradation,[5–7] ultrasonic degradation,[8–11] photo-degradation,[12–15] electro/AIS/PS process,[16] and adsorption.[17–27] The adsorption process has attracted worldwide attention due to its simple implementation and low operation cost. The reported adsorbents include carbons activated by KOH, HNO_3 H_3PO_4 and $ZnCl_2$,[17] olive wood biosorbents,[18] UiO-66-NH_2,[19] glycidyl methacrylate grafted cotton cellulose,[20] yellow bentonite,[21] XAD-4 resin,[22] activated carbon fibers,[23] layered double hydroxides and their calcined products,[24] carbon nanospheres,[25] date seeds[26] and active carbon.[27]

In recent years, ionic liquid-modified silicas (IL-silicas) as adsorbents have been widely used to remove Cu(II), Fe(III), Mn(II) and Ni(II),[28] Pb(II),[29–31] Cr(III,VI),[32–34] lanthanides and scandium ions,[35] oxymatrine,[36] bovine serum albumin,[37] racemic amino acids,[28] thiophenic sulfur compounds,[38] anionic dye,[39,40] dibenzothiophene[41] and phenolic compounds (4-chlorophenol,[42] polyphenols,[43] phenolic acids,[44] naphthols,[45] bisphenol A[46] and 2,4-DNP[47–49]). To elucidate the relation between the structure of IL-silicas and their adsorption performance for phenolic compounds, a series of IL-silicas were designed by varying substituents, the functional groups of the imidazolium ring, counter ions and silane-coupling agents. For the adsorption of 2,4-DNP, 10 imidazolium-modified silicas were prepared in our group. Methyl group, the substituent of imidazolium ring, affected significantly the adsorption performance.[47] The adsorption ability of 4-methylimidazolium-modified silicas was enhanced with the increase of the hydrophilicity of counter anions (BF_4^-. PF_6^-, Tf_2N^-).[48] Amino group also increased significantly the adsorption performance of

[a]*School of Environment, Henan Normal University, Xinxiang 453007, China. E-mail: wzk@htu.cn*

[b]*School of Chemistry and Chemical Engineering, Henan Key Laboratory for Environmental Pollution Control, Key Laboratory for Yellow River and Huai River Water Environment and Pollution Control, Ministry of Education, Henan Normal University, Xinxiang 453007, China*

† Electronic supplementary information (ESI) available. See DOI: 10.1039/c9ra07635b

imidazole-modified silicas. However, the adsorption ability of the adsorbent prepared using 3-mercaptopropyltrimethoxysilane as the coupling agent decreased significantly.[49] In order to overcome the negative effects of coexisting anions on the adsorptive removals of naphthols, a silica adsorbent was prepared through the co-modification of 1-vinyl-3-octadecylimidazolium cations and *p*-styrenesulphonate anions on silica *via* click chemistry reaction.[45] In addition, imidazole, phenyl and hexadecyl were further co-immobilized onto silica *via* silane coupling reaction or thiol–ene click chemistry for bisphenol A adsorption from high salt aqueous solutions.[46] The review of literatures showed that one imidazolium-based ionic liquid was often used to prepare the IL-silicas *via* silane coupling reaction. To the best of our knowledge, two kinds of ionic liquids with imidazole ring containing different substituents were seldom used to simultaneously modify the silica.

In this work, by introducing a series of typical substituent groups including *N*,*N*-dimethylaminopropyl (A), benzyl (B), dodecyl (D) and naphthylmethyl (N) of imidazole ring (Im), the prepared SilprAImCl, SilprBImCl, SilprNImCl, SilprDBImCl and SilprDAImCl (Fig. 1) were applied to further investigate the contribution of interactions between these adsorbents and 2,4-DNP with a particular focus on hydrophobicity interaction, π–π interaction, electrostatic interaction and acid–basic interaction. Our objective is to build the relationship between adsorbent structure and their adsorption performance for 2,4-DNP, and thus guide for designing high efficient adsorbents for removal of phenols from water environment.

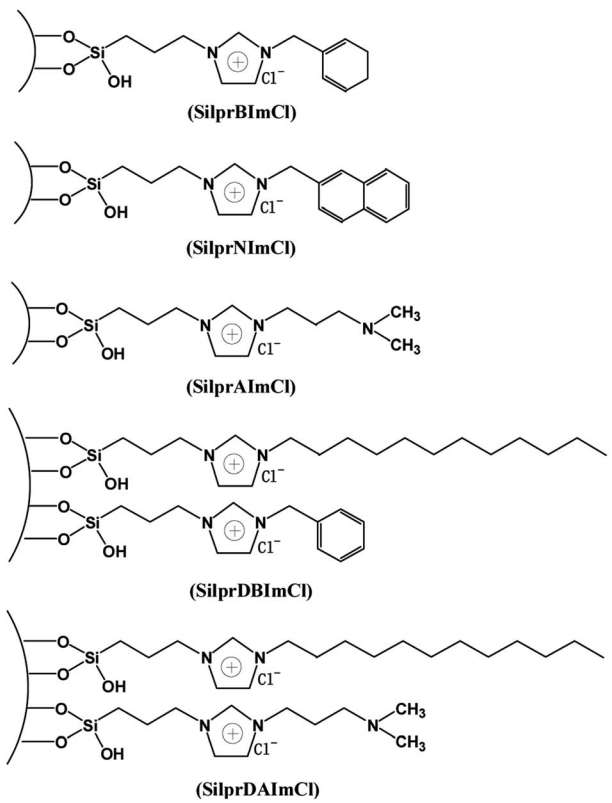

Fig. 1 Structures of the prepared SilprAImCl, SilprBImCl, SilprNImCl, SilprDBImCl and SilprDAImCl.

2. Experimental

2.1 Materials

Imidazole (99%), 3-chloropropyltriethoxysilane (98%), 1-bromododecane (98%) and sodium hydride (60%) were purchased from Aladdin Chemistry Co. Ltd. 2,4-DNP, silica gel (200–300 mesh), 1-benzylimidazole (98%), 1,4-dioxane, triethylamine, ethanol, methanol, magnesium (99.0%) and calcium chloride were obtained from Sinopharm Chemical Reagent Co., Ltd. 1-Chloromethylnaphthalene (97%) and dimethylaminopropylchloride hydrochloride (96%) were obtained from Sigma-Aldrich. Dry toluene and activated silica were obtained using the same procedure reported in the literature.[46] Dry 1,4-dioxane was obtained using the similar method for dry toluene. Oil-free sodium hydride was obtained by washing sodium hydride (60%) thoroughly with petroleum ether. Dry ethanol was obtained through the following method: 1.5 g magnesium, 0.15 g iodine and 15 mL ethanol were added into a round bottom flask and heated until the iodine was dissolved. Then, 250 mL ethanol was added. After the mixture was refluxed for 4–6 h, dry ethanol was obtained by distilment.

2.2 Preparation of SilprBImCl, SilprNImCl, SilprAImCl, SilprDBImCl and SilprDAImCl

The synthesis procedures of SilprBImCl, SilprNImCl and SilprAImCl were shown in Fig. S1 (ESI†), respectively.

2.2.1 Preparation of SilprBImCl. Briefly, 4.0 g 1-benzylimidazole and 6.7 g 3-chloropropyltriethoxysilane were mixed at 80 °C for 24 h, (3-(1-benzyl imidazolyl)propyl)triethoxysilane (product (1)) was obtained. Then, 4.0 g product (1), 5.0 g activated silica and 60 mL dry toluene were mixed at 120 °C for another 24 h. After cooling to room temperature, the mixture was filtrated and washed in turn with toluene, ethanol and deionized water. The SilprBImCl were dried at 60 °C for 10 h.

2.2.2 Preparation of SilprNImCl. 1-(1-Naphthylmethyl) imidazole was synthesized according to the literature.[50] 2.119 g imidazole dissolved in 50 mL dry 1,4-dioxane was added to 100 mL dry 1,4-dioxane containing 1.364 g oil-free sodium hydride. After stirring at 90 °C for 1 h, a solution of 5.0 g 1-chloromethylnaphthalene in 50 mL dry 1,4-dioxane was added dropwise to the above mixtures and stirred at 90 °C for 22 h. Then, the solvent was removed and 100 mL water was added to the residue. Finally, the obtained solution was extracted by dichloromethane and the organic layer was dried with anhydrous magnesium sulfate. 1-(1-Naphthylmethyl)imidazole was obtained after removal of dichloromethane. (3-(1-(1-Naphthylmethyl)imidazolyl)propyl)triethoxysilane (product (2)) was obtained through the reaction of 3-chloropropyltriethoxysilane and 1-(1-naphthylmethyl)imidazole (molar ratio: 1 : 1.2) at 80 °C for 24 h. Then, 4.2 g product (2), 5 g activated silica and 60 mL dry toluene were mixed at 120 °C for 24 h. After cooling to room temperature, the mixture was filtrated and washed in turn with toluene, dichloromethane, ethanol and deionized water. Finally, the SilprNImCl were dried at 60 °C for 24 h.

2.2.3 Preparation of SilprAImCl. SilprAImCl was synthesized according to the literature with some modifications.[51] 5 g SilprImCl prepared previously in our group,[47] 3 g *N*,*N*-dimethylaminopropylchloride hydrochloride and 100 mL ethanol were stirred at 90 °C for 24 h. After cooling to room temperature, the mixture was filtrated and washed with ethanol. Then, the SilprAImCl were dried at 60 °C for 10 h.

The synthesis procedures of SilprDBImCl and SilprDAImCl were shown in (A) and (B) of Fig. S2 (ESI†), respectively.

2.2.4 Preparation of (3-(1-dodecylimidazolyl) propyl) triethoxysilane (product (3)). 1-Dodecylimidazole was prepared according to the literature.[52] In brief, 5.06 g triethylamine, 12.46 g 1-bromododecane and 50 mL dry toluene were added into a dry round bottom flask containing a PTFE-coated magnetic stir bar. After the mixture was stirred at room temperature for 15 min, 3.4 g imidazole was added over 10 min while stirring. Then, the mixture was stirred at 120 °C for 2 h. After cooling to room temperature, the mixture was filtrated and the filtrate was concentrated under reduced pressure to give 1-dodecylimidazole. After that, 3-chloropropyltriethoxysilane and 1-dodecylimidazole (molar ratio: 1 : 1) was stirred at 80 °C for 24 h, product (3) was obtained.

2.2.5 Preparation of ((3-(1-(*N*,*N*-dimethylaminopropyl)) imidazolyl)propyl)triethoxysilane (product (4)). Firstly, 2.04 g imidazole, 4.74 g *N*,*N*-dimethylaminopropylchloride hydrochloride and 30 mL dry ethanol were added into a dry round bottom flask and stirred at 80 °C for 24 h under nitrogen atmosphere. After cooling to room temperature, any remaining volatiles were removed by vacuum rotary evaporation. Then, some water was added and the pH value of the system was adjusted to 8–9 by the addition of 0.1 M NaOH. After that, the mixture was concentrated under reduced pressure and the white residue was dissolved in ethanol. The solution was filtrated and concentrated under reduced pressure. Then, 1-(*N*,*N*-dimethylaminopropyl)imidazole was dried at 80 °C for 24 h. Secondly, 3.6 g 1-(*N*,*N*-dimethylaminopropyl)imidazole, 4.58 g 3-chloropropyltriethoxysilane and 15 mL dry ethanol were added into a dry round bottom flask and stirred at 80 °C for 24 h. Product (4) was obtained after removal of any remaining volatiles by vacuum rotary evaporation.

2.2.6 Preparation of SilprDBImCl. 6 g activated silica and 40 mL dry toluene were added into a dry round bottom flask containing a PTFE-coated magnetic stir bar. Then, 20 mL dry toluene solutions containing 5.99 g product (1) and 7.16 g product (3) were added dropwise to the above mixture. The mixture was stirred at 120 °C for 24 h. After cooling to room temperature, the reactant mixture was filtrated and washed in turn with toluene, ethanol and deionized water. Then, 1-dodecylimidazolium and 1-benzylimidazolium co-modified silicas, SilprDBImCl, were dried at 60 °C for 10 h.

2.2.7 Preparation of SilprDAImCl. 6 g activated silica and 40 mL dry ethanol were added into a dry round bottom flask containing a PTFE-coated magnetic stir bar. Then, 20 mL dry ethanol solutions containing 7.16 g product (3) and 5.96 g product (4) were added dropwise to the above mixture. The mixture was stirred at 90 °C for 24 h. After cooling to room temperature, the reactant mixture was filtrated and washed in turn with ethanol and deionized water. Then, 1-dodecylimidazolium and 1-(*N*,*N*-dimethylaminopropyl) imidazolium co-modified silicas, SilprDAImCl, were dried at 60 °C for 10 h.

2.3 Characterization

Elemental analysis and Fourier transform infrared (FT-IR) spectra were performed on a Vario EL elemental analyzer (Germany) and on a Perkin-Elmer-983 IR spectrophotometer, respectively. Thermogravimetric analysis (STA449C, Netzsch, Germany) was performed with a heating rate of 10 °C min under nitrogen. N_2 adsorption–desorption experiments were carried out on a Quantachrome NOVA 2000e sorption analyzer at liquid nitrogen temperature (77 K). The specific surface area (S_{BET}) was estimated by the linear part of the Brunauer–Emmett–Teller (BET) equation,[53] and the pore size distribution was calculated by the Barrett–Joyner–Halenda (BJH) method.[54]

2.4 Adsorption and desorption experiments

The stock solutions of 2,4-DNP were prepared by dissolving 2,4-DNP in deionized water. 0.1 M HCl or 0.1 M NaOH were used to adjust the pH values of the 2,4-DNP solutions. A UV/visible spectrophotometer (UV-5100, Shanghai Metash Instruments Co. Ltd., China) was used to determine the concentration of 2,4-DNP. All adsorption and desorption experiments were conducted using the same method in our previous reports.[47–49]

3. Results and discussion

3.1 Characterization

The FT-IR spectra in Fig. 2 showed that the typical peaks of Si–O–Si were observed around 465, 796 and 1090 cm^{-1}.[29] The characteristic absorption peaks of imidazole ring (1565 cm^{-1}) were observed.[33,55] The peaks at 1391 and 1448 cm^{-1} were due to the naphthalene ring characteristic vibration.[56] The peaks at 1459 and 1489 cm^{-1} were assigned to the benzene ring characteristic vibration.[57] The peak at 713 cm^{-1} was assigned to C–H vibration, the peak at 2892 cm^{-1} was assigned to the presence of methyl groups. The peaks at 2855 and 2931 cm^{-1} were due to the C–H stretching of the tetrahedral carbon.

The five adsorbents were further analyzed by N_2 adsorption–desorption isotherm at 77 K and the corresponding physical properties including BET surface area, pore size and pore volume were listed in Table 1. It can be seen from Fig. 3 that the five adsorbents showed Type IV N_2 adsorption–desorption isotherms with a hysteresis loop according to the IUPAC classification[58] and the pore size distributions were uniform.

The carbon, hydrogen and nitrogen contents of the five adsorbents by Elemental analysis were presented in Table 2. The thermogravimetric curves (Fig. 4) further provided the content of functional groups and the thermal stability of the five adsorbents. It can be seen from this figure that and the weight losses of SilprBImCl, SilprNImCl, SilprAImCl, SilprDBImCl and

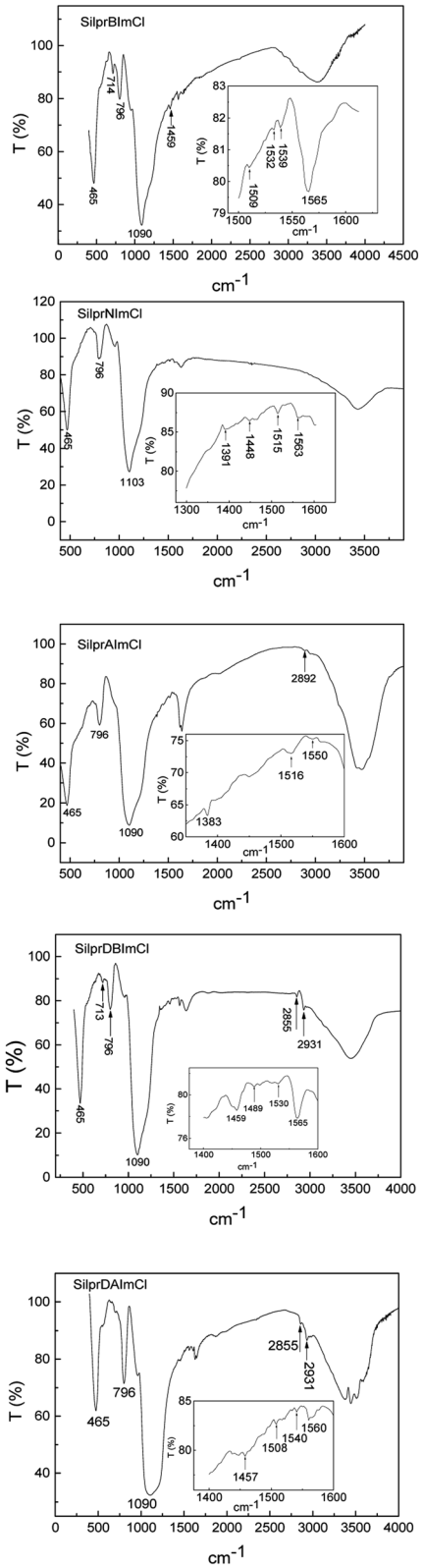

Fig. 2 FTIR spectra of SilprBImCl, SilprNImCl, SilprAImCl, SilprDBImCl and SilprDAImCl.

Table 1 Structural parameters of the five adsorbents

Samples	BET surface area ($m^2\ g^{-1}$)	Total pore volume ($cm^3\ g^{-1}$)	Average pore width (nm)
SilprBImCl	48	0.04	3.61
SilprNImCl	218	0.40	7.26
SilprAImCl	219	0.46	8.46
SilprDBImCl	225	0.43	7.71
SilprDAImCl	291	0.61	8.44

SilprDAImCl between 200 and 600 °C were 17.9%, 16.5%, 12.2%, 17.3% and 9.6%, respectively.

3.2 Adsorption kinetics, isotherms and thermodynamic analysis

To investigate the influence of shaking time, 25 mg SilprBImCl, SilprNImCl, SilprAImCl, SilprDBImCl and SilprDAImCl were added to 50 mL of 2,4-DNP solution with an initial concentration of 50 mg L^{-1} at pH 4.0, 160 rpm and 30 °C, respectively (Fig. 5). It is evident that the adsorption processes reached equilibrium after 780 min for SilprBImCl and 40 min for the other four adsorbents. The SilprBImCl had the longest adsorption equilibrium time among the five prepared adsorbents. This is attributed to its lowest values of total pore volume and average pore width (Table 1), which can inhibit the diffusion process of 2,4-DNP between solid–liquid interface. As shown in Fig. 5, for the three mono immobilization of imidazolium ionic liquids modified silicas, the adsorption capacity of 2,4-DNP increased in order: SilprNImCl > SilprAImCl > SilprBImCl, demonstrating that the naphthylmethyl of imidazole ring on the contributions of the adsorbate–adsorbent interactions was the highest, followed by *N*,*N*-dimethylaminopropyl and benzyl. For the two co-immobilization of imidazolium ionic liquids modified silicas, the SilprDBImCl had the largest adsorption capacity of 2,4-DNP and the SilprDAImCl had the lowest among the five adsorbents. It can be said that the combination of dodecyl and *N*,*N*-dimethylaminopropyl of SilprDAImCl resulted in a negative effect for the adsorption of 2,4-DNP, while the combination of dodecyl and benzyl of SilprDBImCl enhanced significantly the adsorption capacity of 2,4-DNP. The data in Fig. 5 were further analyzed using the pseudo-first-order (eqn (1)), the pseudo-second-order (eqn (2)) and intraparticle diffusion kinetic models (eqn (3)), respectively.[20,29]

$$Q_t = Q_e(1 - \exp(-k_1 t)) \quad (1)$$

$$Q_t = \frac{t}{\frac{1}{k_2 Q_e^{\,2}} + \frac{t}{Q_e}} \quad (2)$$

$$Q_t = k_3\sqrt{t} + C \quad (3)$$

where Q_e (mg g^{-1}) and Q_t (mg g^{-1}) represent the adsorption capacity of 2,4-DNP at equilibrium and any time t, respectively (mg g^{-1}); k_1 (min^{-1}), k_2 (g mg^{-1} min^{-1}) and k_3 (mg g^{-1} $min^{-1/2}$)

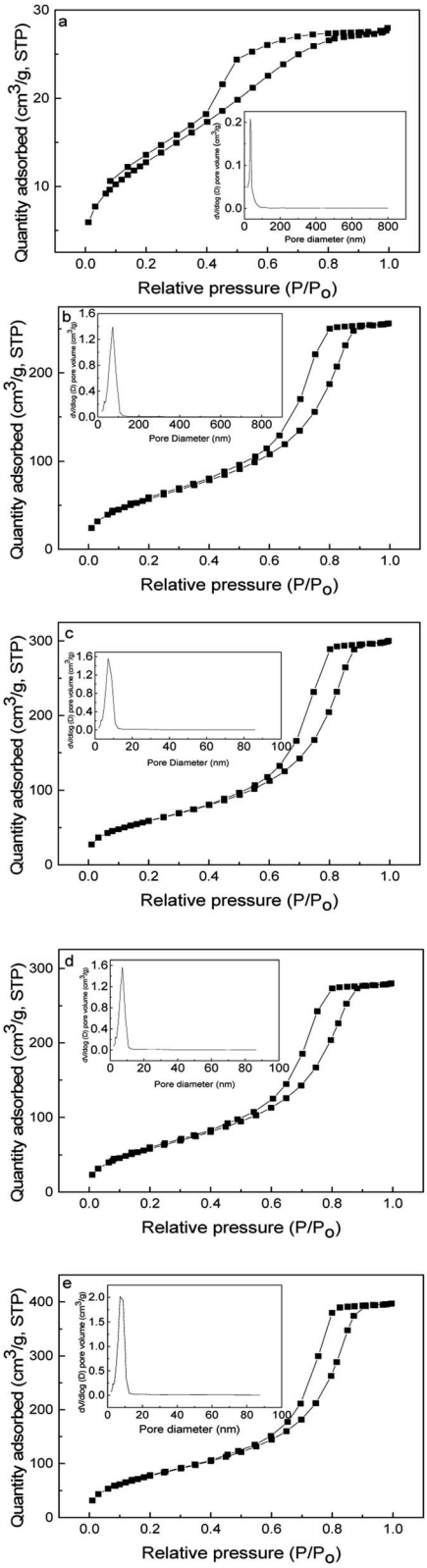

Fig. 3 N_2 adsorption–desorption isotherms and pore size distributions of SilprBImCl (a), SilprNImCl (b), SilprAImCl (c), SilprDBImCl (d) and SilprDAImCl (e).

Table 2 Elemental analysis of the five adsorbents

Samples	C (%)	H (%)	N (%)
SilprBImCl	14.3	2.2	2.3
SilprNImCl	12.4	1.8	1.7
SilprAImCl	7.7	1.7	2.5
SilprDBImCl	11.9	2.0	1.9
SilprDAImCl	6.4	1.5	0.9

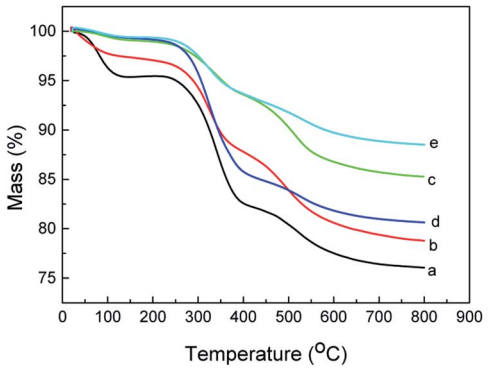

Fig. 4 Thermogravimetric curves of SilprBImCl (a), SilprNImCl (b), SilprAImCl (c), SilprDBImCl (d) and SilprDAImCl (e).

are the rate constant of the pseudo-first-order model, the pseudo-second-order model and the intraparticle diffusion model, respectively. C (mg g^{-1}) is a constant.

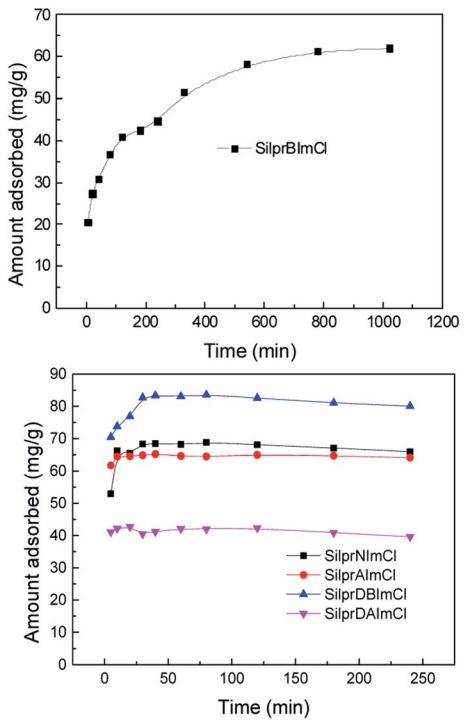

Fig. 5 Effect of shaking time on the adsorption of 2,4-DNP onto the five adsorbents.

Table 3 Parameters of pseudo-second order kinetic model for the adsorption of 2,4-DNP

	Adsorbents				
Parameters	SilprBImCl	SilprNImCl	SilprAImCl	SilprDBImCl	SilprDAImCl
$Q_{e(exp)}$ (mg g^{-1})	61.9	68.8	65.2	83.6	42.7
k_2 (g mg^{-1} min^{-1})	0.00026	0.0222	0.1229	0.02722	0.0531
$Q_{e(cal)}$ (mg g^{-1})	64.7	68.8	64.9	83.7	42.3
R^2	0.9927	0.9998	0.9999	0.9999	0.9998

Table 3 showed that the values of $Q_{e(cal)}$ calculated by eqn (2) were in agreement with those $Q_{e(exp)}$ and the correlation coefficients (R^2) were over 0.99, which highlighted the applicability of the pseudo-second-order adsorption kinetic model for the adsorption of 2,4-DNP onto the five adsorbents.

The adsorption equilibrium of 2,4-DNP was investigated over a range of concentration of 5–100 mg L^{-1} at 30 °C by plotting the equilibrium adsorption capacity of 2,4-DNP onto each adsorbent (Q_e, mg g^{-1}) *versus* the equilibrium concentration of 2,4-DNP. The results were shown in Fig. 6. The equilibrium adsorption data were further analyzed by the most common Langmuir (eqn (4).) and Freundlich (eqn (5)) models, respectively.[55]

$$Q_e = \frac{Q_m b C_e}{1 + b C_e} \quad (4)$$

$$Q_e = K_F C_e^{1/n} \quad (5)$$

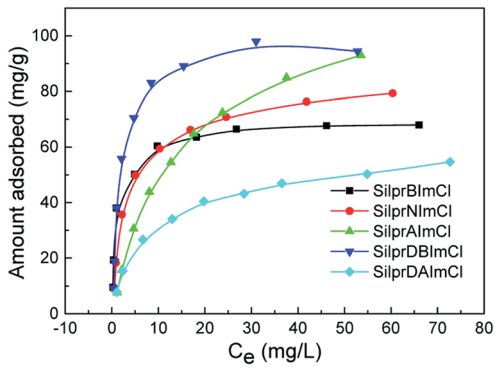

Fig. 6 Adsorption isotherms of 2,4-DNP onto the five adsorbents.

where Q_m is the monolayer adsorption capacity (mg g^{-1}); b is the Langmuir constant; K_F and $1/n$ are the constant indicative of the relative adsorption capacity of the adsorbent and the constant indicative of the heterogeneity factor of Freundlich adsorption isotherm, respectively.

The Langmuir and Freundlich parameters were calculated using the nonlinear optimization method (Table 4). The equilibrium adsorption data were well described by Langmuir according to the value of correlation coefficient (R^2). The Langmuir maximum adsorption capacity for the five adsorbents followed the order: SilprAImCl > SilprDBImCl > SilprNImCl > SilprBImCl > SilprDAImCl. Compared with other adsorbents such as granular activated carbons impregnated with phosphoric acid (299.6 mg g^{-1}),[17] UiO-66-NH_2 (29.6 mg g^{-1}),[19] carbon nanospheres (32.9 mg g^{-1}),[25] SilprImCl (33.3 mg g^{-1}), SilprM_1ImCl (33.9 mg g^{-1}), SilprM_2ImCl (35.9 mg g^{-1}), SilprM_4ImCl (37 mg g^{-1}), SilprM_1M_2ImCl (35.3 mg g^{-1}),[47] SilprP_3NImBr (91.74 mg g^{-1}) and SilprSP_3NImBr (51.81 mg g^{-1}),[49] the five adsorbents in this study possessed a high 2,4-DNP adsorption capacity.

The thermodynamic properties of the five adsorbents for the adsorption of 2,4-DNP were explored at 25, 30, 35, 40, 45 and 50 °C (Fig. 7). The related thermodynamic parameters such as Gibbs free energy change (ΔG), enthalpy change (ΔH) and entropy change (ΔS) were further calculated by the following equations.[20,23]

$$K = \frac{Q_e}{C_e} \quad (6)$$

$$\Delta G = -RT \ln K \quad (7)$$

$$\ln K = \frac{\Delta S}{R} - \frac{\Delta H}{RT} \quad (8)$$

Table 4 Langmuir and Freundlich isotherm constants

		Adsorbents				
Models	Parameters	SilprBImCl	SilprNImCl	SilprAImCl	SilprDBImCl	SilprDAImCl
Langmuir	Q_m (mg g^{-1})	67.5	81.2	116.3	101.6	57.9
	b (L mg^{-1})	1.0094	0.3096	0.0719	0.4929	0.1229
	R^2	0.9784	0.9922	0.9989	0.9836	0.9889
Freundlich	K_F (mg g^{-1}) (mg L^{-1})^n	32.1	26.8	15.4	39.0	13.1
	$1/n$	0.2070	0.2877	0.4682	0.2623	0.3442
	R^2	0.8511	0.8989	0.9618	0.8107	0.9583

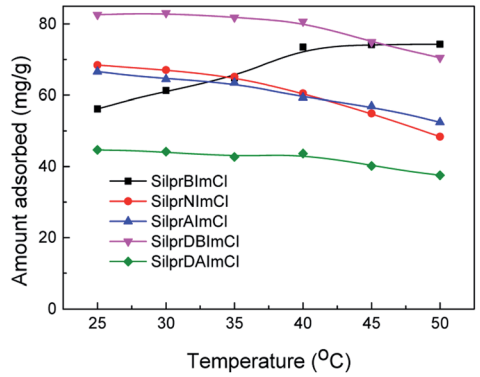

Fig. 7 Effect of temperature on the adsorption of 2,4-DNP onto the five adsorbents.

where K is the distribution coefficient, T (K) is the absolute temperature and R is the ideal gas constant (8.314 J mol^{-1} K^{-1}).

The obtained thermodynamic parameters were listed in Table 5. Firstly, each adsorbent presented a negative value of ΔG, which indicated that the adsorption reactions were spontaneous process and thermodynamically favourable. Secondly, an interesting observation was that the value of ΔH for 2,4-DNP adsorption onto SilprBImCl was positive while the rest were negative for the other four adsorbents. The positive value of ΔH suggested an endothermic adsorption for 2,4-DNP onto SilprBImCl. As Fig. 7 showed, the adsorption capacity of 2,4-DNP onto SilprBImCl increased with increasing temperature from 25 to 50 °C because of its lowest values of total pore volume and average pore width, and higher temperature was favour for the mass transfer of 2,4-DNP. The similar results were also reported in different adsorption systems such as the adsorption of catechol onto montmorillonite modified with two hydroxyl-containing Gemini surfactants[59] and the adsorption of 4-nitrotoluene-2-sulfonic acid onto two magnetic resins at higher concentrations.[60] In addition, the obtained negative values of ΔH suggested an exothermic adsorption for 2,4-DNP on the other four adsorbents, since these adsorbents had larger BET surface area compared with SilprBImCl. 2,4-DNP could easily approach active sites of these adsorbents and temperature was not the main factor influencing the adsorption of 2,4-DNP. The observations obtained in this work agreed well with the published results such as the adsorption of *p*-nitroaniline onto polymeric adsorbents[61] and the adsorption of 2,4-dichlorophenol onto cyclodextrin-ionic liquid polymer.[62]

3.3 Adsorption mechanism

To further clarify the adsorption process of 2,4-DNP onto the five adsorbents, the effects of competitive anions were studied by adding NaCl or $NaNO_3$ solutions with different concentrations from 0.005 to 0.1 mol L^{-1} into the corresponding adsorption system. As shown in Fig. 8, the adsorption capacity of 2,4-DNP onto the five adsorbents decreased significantly with the increase of NaCl or $NaNO_3$ concentrations, which indicated the occurrence of the competition adsorptions between 2,4-DNP and anions. These interesting results confirmed that the five adsorbents kept electrostatic nature.

The effects of pH on the adsorption process were carried out from pH 2 to 10 (Fig. 9). For the SilprNImCl, SilprDBImCl and

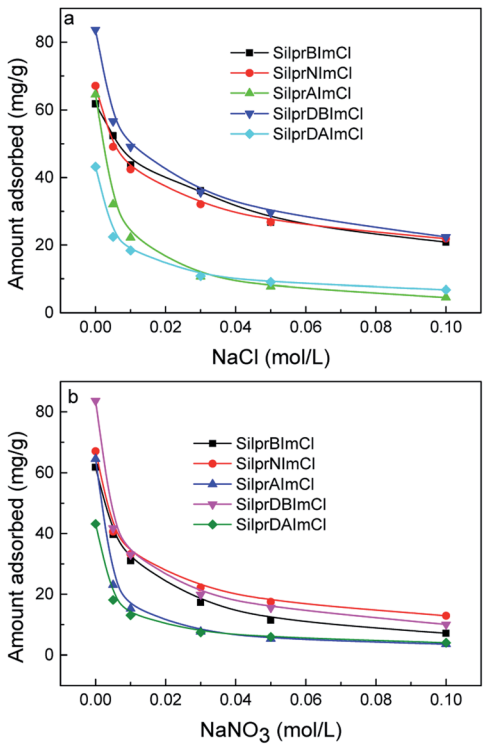

Fig. 8 Effect of NaCl (a) and $NaNO_3$ (b) on the adsorption of 2,4-DNP onto the five adsorbents.

Table 5 Thermodynamic parameters for the adsorption of 2,4-DNP

Adsorbents	ΔH (kJ mol^{-1})	ΔS (kJ mol^{-1} K^{-1})	ΔG (kJ mol^{-1})					
			25 °C	30 °C	35 °C	40 °C	45 °C	50 °C
SilprBImCl	28.8	0.1620	−19.4	−20.3	−21.0	−22.4	−22.9	−23.3
SilprNImCl	−26.9	−0.0199	−20.7	−20.9	−21.1	−20.9	−20.6	−20.2
SilprAImCl	−18.6	0.0068	−20.5	−20.6	−20.9	−20.8	−20.8	−20.7
SilprDBImCl	−22.6	0.0015	−22.7	−23.2	−23.3	−23.5	−22.9	−22.7
SilprDAImCl	−8.8	0.0322	−18.3	−18.6	−18.7	−19.1	−19.0	−19.0

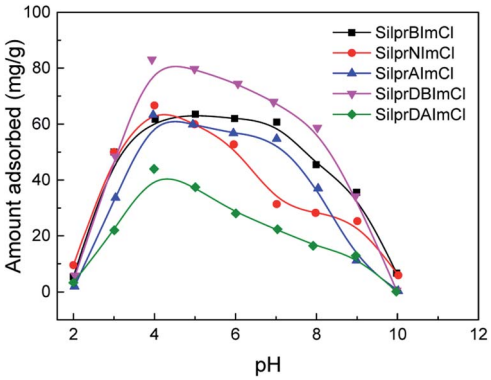

Fig. 9 Effect of pH on the adsorption of 2,4-DNP onto the five adsorbents.

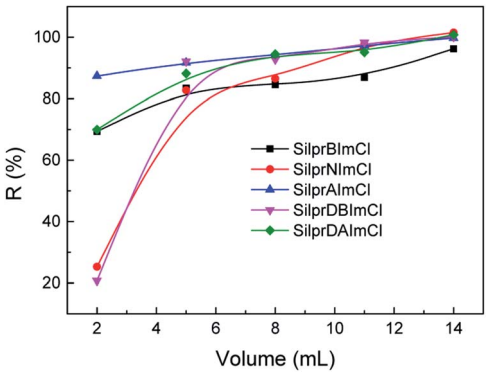

Fig. 10 Effect of volume of 0.5 mol L^{-1} HCl on the recovery of 2,4-DNP.

SilprDAImCl, the adsorption capacity of 2,4-DNP onto the three adsorbents increased significantly with the pH value from 2 to 3.95 and began to decrease significantly with further increase of the pH values. This can be attributed to the competition effects between 2,4-DNP and OH^- ions at higher pH. However, for the SilprBImCl and SilprAImCl, the adsorption capacity for 2,4-DNP kept a platform in the pH range of 4–7. It was evident that SilprDBImCl exhibited the highest adsorption performance for 2,4-DNP in the pH range of 4–8 among the five adsorbent. The adsorption capacities of 2,4-DNP onto SilprBImCl, SilprNImCl and SilprAImCl at the original pH value (3.95) were 61.8, 66.7 and 63.4 mg g^{-1}, respectively. Compared with the previously synthesized imidazole-modified silica adsorbents in our group,[47] it was concluded that benzyl, naphthylmethyl or dimethylaminopropyl enhanced the adsorption of 2,4-DNP, attributing to the additional interactions such as π–π interaction between the benzyl, naphthylmethyl and 2,4-DNP for SilprBImCl and SilprNImCl, and acid–base interaction between *N*,*N*-dimethylaminopropyl and 2,4-DNP for SilprAImCl.

It was worth noting that SilprDAImCl exhibited the smallest adsorption performance among the five adsorbents, which indicated that the co-modification of silicas with 1-dodecylimidazolium and 1-*N*,*N*-dimethylaminopropylimidazolium was not favorable for the adsorption process. It can be concluded that the combination of hydrophobicity interaction and π–π interaction favours the enhancement of adsorption performance. However, the combination of hydrophobicity interaction and acid–base interaction decreased significantly the adsorption performance. One possible explanation for this phenomenon was that the 2,4-DNP adsorption achieved by acid–base interactions may be hindered due to the directionality and short range of hydrogen bonding.[63] These interesting findings indicated that the contributions of substituent groups of imidazole ring for the adsorption of 2,4-DNP onto ionic liquids-modified silicas was not a simple sum of that of the single substituent group.

3.4 Desorption experiments

Dynamic column desorption experiments were carried out with various volumes (2 to 14 mL) of 0.5 mol L^{-1} HCl and the results were presented in Fig. 10. For the five adsorbents, the recovery (R) increased with increase of HCl volumes from 2 to 14 mL and the recovery was over 96% when the volume of HCl was 14 mL. It was interesting to find when the volume of HCl was 2 mL, the recovery was 25.3% and 20.8% for the SilprNImCl and SilprDBImCl respectively, which was lower than that of the other three adsorbents. This may be attributed to the higher affinity of the two adsorbents for 2,4-DNP resulting in the low recovery.

4. Conclusion

Three mono-immobilization and two co-immobilization of imidazolium ionic liquids modified silicas were successfully fabricated and characterized with regard to the contribution of substituent groups of imidazole ring for the adsorption of 2,4-DNP. Benzyl, naphthylmethyl and *N*,*N*-dimethylaminopropyl of imidazole ring displayed the improved adsorption performance for 2,4-DNP *via* π–π or acid–basic interactions. And the contribution of substituent groups of imidazole ring for the adsorption of 2,4-DNP followed the order: naphthylmethyl > *N*,*N*-dimethylaminopropyl > benzyl. Besides, the SilprDBImCl had the largest adsorption capacity and the SilprDAImCl had the lowest among the five adsorbents. That was to say, the contributions of substituent groups of imidazole ring for the adsorption of 2,4-DNP onto these ionic liquids-modified silicas were not a simple sum of that of the single substituent group.

Conflicts of interest

There are no conflicts to declare.

Acknowledgements

The financial support provided by Natural Science Foundation of Henan province of China (No. 182300410257), the Key Scientific Research Project of Higher Education of Henan Province of China (No. 18A150034) and Science and Technology Department (No. 182102311025) are gratefully acknowledged.

Notes and references

1 Y. Ji, Y. Shi, Y. Yang, P. Yang, L. Wang, J. Lu, J. Li, L. Zhou, C. Ferronato and J. Chovelon, *J. Hazard. Mater.*, 2019, **361**, 152–161.
2 P. Cañizares, C. Sáez, J. Lobato and M. A. Rodrigo, *Electrochim. Acta*, 2004, **49**, 4641–4650.
3 I. M. S. Pillai and A. K. Gupta, *J. Electroanal. Chem.*, 2015, **756**, 108–117.
4 I. M. S. Pillai and A. K. Gupta, *J. Electroanal. Chem.*, 2016, **762**, 66–72.
5 T. Tang, Z. Yue, J. Wang, T. Chen and C. Qing, *J. Hazard. Mater.*, 2018, **343**, 176–180.
6 R. A. Kristanti, T. Toyama, T. Hadibarata, Y. Tanaka and K. Mori, *RSC Adv.*, 2014, **4**, 1616–1621.
7 A. Ghosh, M. Khurana, A. Chauhan, M. Takeo, A. K. Chakraborti and R. K. Jain, *Environ. Sci. Technol.*, 2010, **44**, 1069–1077.
8 Z. Guo, R. Feng, J. Li, Z. Zheng and Y. Zheng, *J. Hazard. Mater.*, 2008, **158**, 164–169.
9 Z. Guo, Z. Zheng, S. Zheng, W. Hu and R. Feng, *Ultrason. Sonochem.*, 2005, **12**, 461–465.
10 M. V. Bagal, B. J. Lele and P. R. Gogate, *Ultrason. Sonochem.*, 2013, **20**, 1217–1225.
11 M. V. Bagal and P. R. Gogate, *Ind. Eng. Chem. Res.*, 2013, **52**, 8386–8391.
12 H. Bashir, X. Yi, J. Yuan, K. Yin and S. Luo, *J. Photochem. Photobiol., A*, 2019, **382**, 111930.
13 P. Shandilyaa, D. Mittalb, A. Sudhaika, M. Sonic, P. Raizadaa, A. K. Saini and P. Singh, *Sep. Purif. Technol.*, 2019, **210**, 804–816.
14 Q. He, Y. Ni and S. Ye, *RSC Adv.*, 2017, **7**, 27089–27099.
15 X. Zhou, C. Lai, D. Huang, G. Zeng, L. Chen, L. Qin, P. Xu, M. Cheng, C. Huang, C. Zhang and C. Zhou, *J. Hazard. Mater.*, 2018, **346**, 113–123.
16 J. Li, Y. Ren, L. Lai and B. Lai, *J. Hazard. Mater.*, 2018, **344**, 778–787.
17 A. M. Carvajal-Bernal, F. Gómez and L. Giraldo, *Microporous Mesoporous Mater.*, 2015, **209**, 150–156.
18 A. H. EI-Sheikh, A. P. Newman, A. J. Said, A. M. Alzawahreh and M. M. Abu-Helal, *J. Environ. Manage.*, 2013, **118**, 1–10.
19 Z. Xu, Y. Wen, L. Tian and G. Li, *Inorg. Chem. Commun.*, 2017, **77**, 11–13.
20 E. Vismara, L. Melone, G. Gastaldi, C. Cosentino and G. Torri, *J. Hazard. Mater.*, 2009, **170**, 798–808.
21 Z. Yaneva and B. Koumanova, *J. Colloid Interface Sci.*, 2006, **293**, 303–311.
22 Y. Ku and K. Lee, *J. Hazard. Mater.*, 2000, **80**, 59–68.
23 Q. Liu, T. Zheng, P. Wang, J. Jiang and N. Li, *Chem. Eng. J.*, 2010, **157**, 348–356.
24 D. Chaara, I. Pavlovic, F. Bruna, M. A. Ulibarri, K. Draoui and C. Barriga, *Appl. Clay Sci.*, 2010, **50**, 292–298.
25 J. C. Lazo-Cannata, A. Nieto-Márquez, A. Jacoby, A. L. Paredes-Doig, A. Romero, M. R. Sun-Kou and J. L. Valverde, *Sep. Purif. Technol.*, 2011, **80**, 217–224.
26 N. Z. Al-Mutairi, *Desalination*, 2010, **250**, 892–901.
27 K. A. Krishnan, S. S. Suresh, S. Arya and K. G. Sreejalekshmi, *Desalin. Water Treat.*, 2015, **54**, 1850–1861.
28 G. Qian, H. Song and S. Yao, *J. Chromatogr. A*, 2016, **1429**, 127–133.
29 B. Ekka, L. Rout, M. K. S. A. Kumar, R. K. Patel and P. Dash, *J. Environ. Chem. Eng.*, 2015, **3**, 1356–1364.
30 M. E. Mahmoud, *Desalination*, 2011, **266**, 119–127.
31 M. E. Mahmoud and H. M. Al-Bishri, *Chem. Eng. J.*, 2011, **166**, 157–167.
32 Y. Liu, L. Guo, L. Zhu, X. Sun and J. Chen, *Chem. Eng. J.*, 2010, **158**, 108–114.
33 Z. Wang, C. Ye, X. Wang and J. Li, *Appl. Surf. Sci.*, 2013, **287**, 232–241.
34 Y. Zhang, H. Wang, N. Sun and R. Chi, *Sep. Purif. Technol.*, 2018, **205**, 84–93.
35 A. N. Turanov, V. K. Karandashev, N. S. Sukhinina, V. M. Masalov and G. A. Emelchenko, *J. Environ. Chem. Eng.*, 2016, **4**, 3788–3796.
36 W. Bi, M. Tian and K. H. Row, *J. Chromatogr. B: Anal. Technol. Biomed. Life Sci.*, 2012, **880**, 108–113.
37 H. Song, C. Yang, A. Yohannes and S. Yao, *RSC Adv.*, 2016, **6**, 107452–107462.
38 F. Wang, Z. Zhang, J. Yang, L. Wang, Y. Lin and Y. Wei, *Fuel*, 2013, **107**, 394–399.
39 M. Zarezadeh-Mehrizi, A. Badiei and A. R. Mehrabadi, *J. Mol. Liq.*, 2013, **180**, 95–100.
40 O. Tkachenko, A. Panteleimonov, I. Padalko, A. Korobov, Y. Gushikem and Y. Kholin, *Chem. Eng. J.*, 2014, **254**, 324–332.
41 J. Zhang, S. Sun, Y. Bian, W. Li, R. Liu and D. Zhao, *Fuel*, 2018, **220**, 513–520.
42 H. M. Marwani and E. M. Bakhsh, *Chem. Eng. J.*, 2017, **326**, 794–802.
43 W. Zhang, X. Feng, Y. Alula and S. Yao, *Food Chem.*, 2017, **230**, 637–648.
44 L. Nie, J. Lu, W. Zhang, A. He and S. Yao, *Sep. Purif. Technol.*, 2015, **155**, 2–12.
45 Z. Wang, C. Ye, L. Chen and H. Wu, *RSC Adv.*, 2017, **7**, 2650–2657.
46 Z. Wang, Y. Zhu, H. Chen, H. Wu and C. Ye, *J. Taiwan Inst. Chem. Eng.*, 2018, **86**, 120–132.
47 Z. Wang, C. Ye, J. Li, H. Wang and H. Zhang, *J. Hazard. Mater.*, 2013, **260**, 955–966.
48 C. Ye, X. Wang, H. Wang and Z. Wang, *J. Taiwan Inst. Chem. Eng.*, 2014, **45**, 2868–2877.
49 Z. Wang, C. Ye and H. Wang, *Int. J. Environ. Sci. Technol.*, 2016, **13**, 113–124.
50 S. Liu, X. Wu, Q. Liu, Z. Zheng, Y. Zang, S. Ge and J. Feng, *Chin. J. Inorg. Chem.*, 2008, **24**, 1444–1449.
51 M. Tian, W. Bi and K. H. Row, *Phytochem. Anal.*, 2013, **24**, 81–86.
52 H. Qiu, Q. Jiang, X. Liu and S. Jiang, *Chromatographia*, 2008, **68**, 167–171.
53 M. Gao, W. Wang, H. Yang and B. Ye, *Chem. Eng. J.*, 2020, **380**, 122459.

54 Z. Wen, J. Lu, Y. Zhang, G. Cheng, S. Huang, J. Chen, R. Xu, Y. Ming, Y. Wang and R. Chen, *J. Hazard. Mater.*, 2020, **383**, 121172.
55 G. Zhu, G. Cheng, T. Lu, Z. Cao, L. Wang, Q. Li and J. Fan, *J. Hazard. Mater.*, 2019, **373**, 347–358.
56 M. Agrawal, V. Deval, A. Gupta, B. R. Sangala and S. S. Prabhu, *Spectrochim. Acta, Part A*, 2016, **167**, 142–156.
57 Y. Jiao, C. Cao and X. Zhao, *J. Mol. Struct.*, 2012, **1027**, 57–63.
58 A. Kara, E. Demirbel, N. Tekin, B. Osman and N. Besirli, *J. Hazard. Mater.*, 2015, **286**, 612–623.
59 Y. Liu, M. Gao, Z. Gu, Z. Luo, Y. Ye and L. Lu, *J. Hazard. Mater.*, 2014, **267**, 71–80.
60 W. Wang, Y. Ma, A. Li, Q. Zhou, W. Zhou and J. Jin, *J. Hazard. Mater.*, 2015, **294**, 158–167.
61 G. Xiao, R. Wen, D. Wei and D. Wu, *J. Hazard. Mater.*, 2014, **280**, 97–103.
62 M. Raoov, S. Mohamad and M. R. Abas, *J. Hazard. Mater.*, 2013, **263**, 501–516.
63 M. C. Xu, Y. Zhou and J. H. Huang, *J. Colloid Interface Sci.*, 2008, **327**, 9–14.